Seismic Analysis of Tall Buildings Through an Enriched Equivalent Beam Model: Application to Grenoble City Hall

Carolina Franco Ariza, Céline Chesnais, Jean-François Semblat, Cédric Desprez and Cedric Giry

March 14, 2022

Seismic analysis of tall buildings through an enriched equivalent beam model: Application to Grenoble City Hall

Franco Carolina - Géodynamique Structure, Immeuble Cap Sud, 106 Avenue Marx Dormoy, 92120 Montrouge, France, carolina.franco@geodynamique.com

Chesnais Céline - GERS-SRO, Univ Gustave Eiffel, IFSTTAR, F-77447 Marne-la-Vallée, France, celine.chesnais@univ-eiffel.fr

Semblat Jean-François - IMSIA (UMR9219), CNRS, EDF, CEA, ENSTA Paris, Institut Polytechnique de Paris, 91120 Palaiseau, France, jean-francois.semblat@ensta-paris.fr

Desprez Cédric - Univ. Lyon, INSA-Lyon, GEOMAS, F-69621, Villeurbanne, France, cedric.desprez@insa-lyon.fr

Giry Cédric - Université Paris-Saclay, ENS Paris-Saclay, CentraleSupélec, CNRS, LMPS - Laboratoire de Mécanique Paris-Saclay, 91190, Gif-sur-Yvette, France, cedric.giry@ens-paris-saclay.fr

Abstract: The seismic assessment of multi-story buildings at city scale requires robust but simplified modeling techniques to reduce the computational resources and time. This paper presents an equivalent beam model (EBM), issued from homogenization, capable of describing the seismic response of real tall buildings. The EBM is a generalization of the Timoshenko beam model. It integrates shear, global bending, and inner bending mechanisms, which are identified to control the response of reticulated structures such as buildings, foams, honeycombs, or lattice structures. The properties of the EBM are obtained through the static analysis of a single building story. This work uses a new finite element formulation of the EBM to estimate the dynamic properties of buildings (i.e., eigenfrequencies and eigenmodes) and perform time history analyses with natural seismic records. This approach is validated through a real case study. The Grenoble City Hall corresponds to a regular 13-story reinforced concrete building located in Grenoble-France. The inner bending significantly influences its behavior, whereas usual beam models do not include this mechanism. The results obtained via this 1D simplified EBM match those obtained with a fully 3D finite element simulation, which are also very close to experimental data.

Keywords: seismic response, tall building, homogenized beam, finite element method

1. Introduction

In seismic assessment studies of a large group of existing buildings, simplified models for dynamic analyses keep being attractive despite the actual calculation capabilities of computers. At the local scale, information such as forces and deformations in the structural elements is of interest. Modal parameters such as natural frequencies and mode shapes are fundamental for the dynamic description at the global scale. The calculation of all the variables at both local and global scales is rarely performed by using a single simplified 1D modeling strategy. However, sophisticated techniques based on homogenization are able to keep the link between different scales.

Two conditions are necessary to apply homogenization to building structures: periodicity and scale separation. The scale separation condition relates the height of one story l_m to the height of the entire building H. The scale separation ratio, $\varepsilon = \frac{\pi l_m}{2H}$ for the first mode, must be sufficiently small to allow homogenization. This condition is respected if the structure has at least five stories. Moreover, ordinary mid-rise and high-rise buildings are frequently periodic in height because a typical story is repeated all along the building height. It is therefore possible to obtain homogenized 1D models for their dynamic characterization (Chesnais, 2010) (Chesnais et al, 2011).

This study is based on the equivalent beam model (EBM), issued from the homogenization method of periodic discrete media (HPDM) (Caillerie, 1989) applied to multi-bay frame structures (Hans et al., 2008)(Chesnais, 2010), and also on its finite element formulation, named the homogenized beam finite element model (HBFEM) (Franco et al., 2022). The HBFEM facilitates time history analyses and the integration of several story properties for non-fully periodic structures made of "periodic sub-structures". Herein, the HBFEM is utilized to perform dynamic analyses of an existing multi-bay frame building. The Grenoble City Hall (GCH) is a 13-story reinforced concrete building monitored since 2004 by the French Accelerometric Network (RAP). The GCH has served as a candidate in multiple research studies dealing with experimental dynamic characterization (Michel et al., 2006), 3D numerical model calibration (Michel et al., 2010) (Desprez, 2010), or fiber reinforced polymer retrofitting assessments (Desprez, 2010). Its building structure is not fully periodic: the structural element sections slightly decrease at mid-height. The HBFEM formulation proposed in (Franco et al., 2022) is used to integrate the properties of the typical stories of the GCH to build its 1D model.

In general, structures modeled with this approach should fulfill the following prerequisites:
- Verically regular in mass, stiffness, and strength to respect the periodicity condition required by the homogenization.
- At least five stories (Hans et al., 2008) to respect the scale separation condition.
- The dynamic characterization must be limited to the analysis of the vibration modes with a sufficiently long wavelength. The maximum number of modes which can be modeled with this approach is approximately $N/3$, where N is the number of stories of the building. This condition is typically valid in earthquake engineering studies where the lowest frequencies are of interest.

In this work, the analysis is focused on the linear elastic framework. The results of the GCH equivalent beam model are compared with those of its full detailed numerical model. The objective is three-fold:
  i) Detail the construction of the HBFEM model for real non-fully periodic structures.
  ii) Demonstrate the capabilities of this simplified model in the computation of dynamic properties and time history analyses.
  iii) Highlight the advantages of the understanding of the mechanical functioning of building structures.

2. Model formulation

The transverse dynamics of building-type structures (interconnected walls/columns and floors/beams) is described through the HPDM by (Boutin et al., 2003) (Hans et al., 2008). They focused on one-bay frame structures as the one shown in Fig.1a. This idealized structure has a total height $H = Nl_m$, where N is the number of stories, l_m the height of the stories and l_p their width. A systematic study on these one-bay frame structures is conducted to assess the evolution of the overall structural behavior with respect to the stiffness contrast between the walls and the floors. Two significant results from this study can be highlighted: the identification of the structure governing mechanisms, and an analytical formulation, named equivalent beam model (EBM), describing the transverse dynamics.

2.1 Governing mechanisms of building-type structures

(Hans et al., 2008) reveals that three mechanisms govern the structural behavior in the transverse direction: the shear of the stories (stiffness K_s), the inner bending (stiffness $\mathcal{K}_i$), and the global bending (stiffness $\mathcal{K}_g$) (Fig.1b). The story shear deformation is generated by the local bending (i.e., between neighboring nodes) of the vertical and/or horizontal elements. For the inner bending mechanism, the vertical elements behave as cantilever bending beams at the structure scale and are synchronized by the horizontal ones. These horizontal elements have a large axial stiffness and bend locally. The global bending mechanism occurs because of the out-of-phase tension-compression of the vertical elements. The relative importance of the mechanisms depends on the stiffness contrast between the vertical and horizontal elements. For example, the inner bending can only appear if the horizontal elements are much more flexible than the vertical ones.

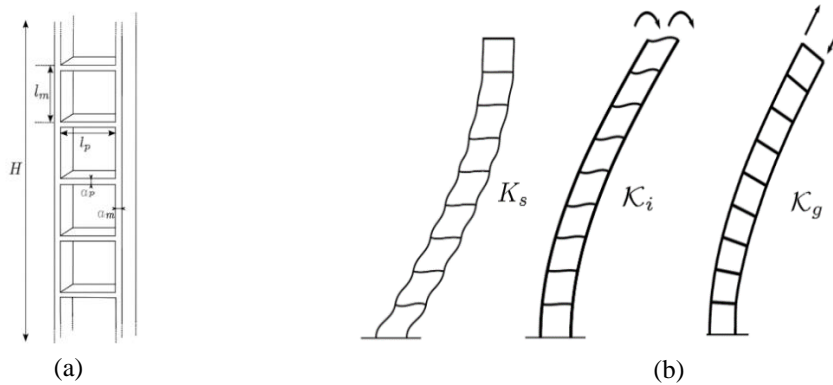(a)   (b)

Fig. 1 (a) Idealized one-bay frame structure studied in (Boutin et al., 2003) (Hans et al., 2008). (b) Mechanisms that govern its transverse behavior.

2.2   Equivalent beam model (EBM) - analytical form

The transverse motion of single frame structures is parametrized by three kinematic variables: the mean transverse displacement, u, the story rotation, α, and the mean nodal rotation, θ. The first two, representing the story rigid body motion, appear explicitly in the global dynamic description of the structure. Conversely, θ, associated with the story deformation, is a hidden variable obtained from the rigid body motion thanks to the internal equilibrium of the story. Fig.2 illustrates the deformed one-bay frame structure and the associated kinematic variables.
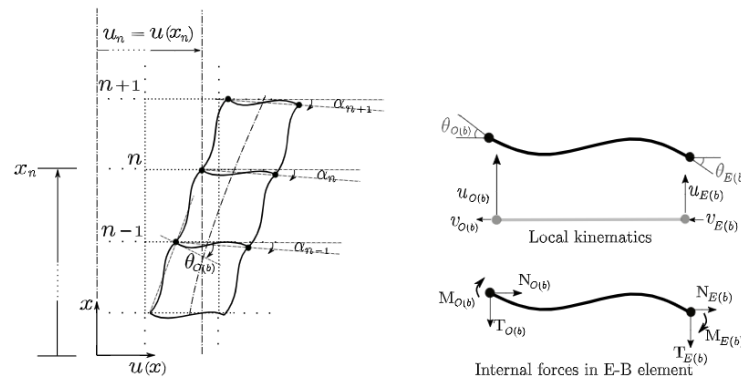

Fig. 2 One-bay frame structure deformation

The three mechanisms governing the transverse vibrations of the EBM are associated with one force and two moments defined by the constitutive laws given in Equations (1) and related by the equilibrium equations (2).

Constitutive laws:

Shear force
(generated by the shear of the stories)
$$T(x,t) = K_s\left(\frac{\partial u(x,t)}{\partial x} - \alpha(x,t)\right)$$

Inner bending moment
$$\mathcal{M}(x,t) = \mathcal{K}_i \frac{\partial^2 u(x,t)}{\partial x^2} \qquad (1)$$

Global bending moment
$$M(x,t) = \mathcal{K}_g \frac{\partial \alpha(x,t)}{\partial x}$$

Equilibrium equations:
$$\mathcal{T}(x,t) = T(x,t) - \frac{\partial \mathcal{M}(x,t)}{\partial x}, \qquad \frac{\partial \mathcal{T}(x,t)}{\partial x} = \Lambda \frac{\partial^2 u(x,t)}{\partial t^2} + f(x,t)$$

$$\frac{\partial M(x,t)}{\partial x} = -T(x,t) \qquad (2)$$

where $\mathcal{T}$ corresponds to the total shear force, $f(x,t)$ is the linear density of the external transverse load, and Λ is the linear mass (mass of the story divided by its height l_m). The combination of these equations, in the harmonic regime ($f(x,t) = 0$), leads to a sixth order differential equation (Hans et al., 2008):

$$\frac{\mathcal{K}_i \mathcal{K}_g}{K_s} \frac{d^6 \hat{u}(x)}{dx^6} - (\mathcal{K}_i + \mathcal{K}_g)\frac{d^4\hat{u}(x)}{dx^4} - \frac{\mathcal{K}_g \Lambda \omega^2}{K_s}\frac{d^2\hat{u}(x)}{dx^2} + \Lambda\omega^2\hat{u}(x) = 0 \qquad (3)$$

where ω is the circular frequency. For a structure clamped at the bottom and free at the top, the boundary conditions are $\hat{u} = 0$, $\frac{d\hat{u}}{dx} = 0$ and $\hat{\alpha}=0$ at $x = 0$ and $\hat{T} = 0$, $\widehat{\mathcal{M}} = 0$ and $\widehat{M} = 0$ at $x = H$. Details on the construction of this equation can be found in (Hans et al., 2008) (Chesnais, 2010). Note that the EBM is an enriched form of the fourth-order Timoshenko beam equation. The higher differential equation order is attributed to an additional kinematic mechanism that may appear under large stiffness contrasts between the story structural elements. This sixth differential equation can degenerate into more simplified beam models (e.g., shear beam or Timoshenko beam) according to the stiffness contrast between structural elements (see (Hans et al., 2008)).

The implementation of the HPDM on two-bay and three- bay frame structures done by (Chesnais, 2010) verifies and encounters these results, and further studies are performed in (Chesnais et al., 2011) (Franco et al., 2019) to extend the EBM applications to real building structures. Comparisons with full finite element models show that the EBM can accurately describe the transverse dynamics of building type structures respecting the aforementioned conditions.

2.3 Equivalent beam model (EBM) - numerical form

Aiming to perform extensive parametric studies, time history analyses, and extend the EBM applications to non-fully periodic structures, (Franco et al., 2022) proposes and verifies a finite element formulation of the EBM built via virtual power formulation principles. The governing equation of the motion is expressed in matrix form as (Franco et al., 2022):

$$\boldsymbol{M}\ddot{E} + \boldsymbol{C}\dot{E}(t) + \boldsymbol{K}E(t) = f(t) \qquad (4)$$

where $\boldsymbol{M}$ $(d \times d)$, $\boldsymbol{C}(d \times d)$, $\boldsymbol{K}(d \times d)$ are the time-invariant mass, damping and stiffness matrices of the structure, respectively. d refers to the number of degrees of freedom. The d-dimensional vector $E(t)$ corresponds to the structural response vector of the transverse motion in terms of u and α at time t; and $f(t)$ is the time dependent excitation force.

The weak formulations of the homogenized beam finite element (HBFEM) lead to the following generalized elementary stiffness K_t and mass M_e matrices:

$$K_t = K_s \begin{bmatrix} \frac{6}{5h_e}+\frac{\mathcal{K}_i}{K_s}\frac{12}{h_e^3} & \frac{\mathcal{K}_i}{K_s}\frac{6}{h_e^2}+\frac{1}{10} & -\frac{6}{5h_e}-\frac{\mathcal{K}_i}{K_s}\frac{12}{h_e^3} & \frac{\mathcal{K}_i}{K_s}\frac{6}{h_e^2}+\frac{1}{10} & \frac{1}{10} & \frac{4}{5} & \frac{1}{10} \\ & \frac{2h_e}{15}+\frac{\mathcal{K}_i}{K_s}\frac{4}{h_e} & -\frac{\mathcal{K}_i}{K_s}\frac{6}{h_e^2}-\frac{1}{10} & \frac{\mathcal{K}_i}{K_s}\frac{2}{h_e}-\frac{h_e}{30} & -\frac{7h_e}{60} & \frac{h_e}{15} & \frac{h_e}{20} \\ & & \frac{6}{5h_e}+\frac{\mathcal{K}_i}{K_s}\frac{12}{h_e^3} & -\frac{\mathcal{K}_i}{K_s}\frac{6}{h_e^2}-\frac{1}{10} & -\frac{1}{10} & -\frac{4}{5} & -\frac{1}{10} \\ & & & \frac{2h_e}{15}+\frac{\mathcal{K}_i}{K_s}\frac{4}{h_e} & \frac{h_e}{20} & \frac{h_e}{15} & -\frac{7h_e}{60} \\ & & \text{SYM} & & \frac{2h_e}{15}+\frac{\mathcal{K}_g}{K_s}\frac{7}{3h_e} & \frac{h_e}{15}-\frac{\mathcal{K}_g}{K_s}\frac{8}{3h_e} & \frac{\mathcal{K}_g}{K_s}\frac{1}{3h_e}-\frac{h_e}{30} \\ & & & & & \frac{8h_e}{15}+\frac{\mathcal{K}_g}{K_s}\frac{16}{3h_e} & \frac{h_e}{15}-\frac{\mathcal{K}_g}{K_s}\frac{8}{3h_e} \\ & & & & & & \frac{2h_e}{15}+\frac{\mathcal{K}_g}{K_s}\frac{7}{3h_e} \end{bmatrix} \quad M_e = \frac{\Lambda h_e}{420}\begin{bmatrix} 156 & 22h_e & 54 & -13h_e & 0 & 0 \\ 22h_e & 4h_e^2 & 13h_e & -3h_e^2 & 0 & 0 \\ 54 & 13h_e & 156 & -22h_e & 0 & 0 \\ -13h_e & -3h_e^2 & -22h_e & 4h_e^2 & 0 & 0 \\ 0 & 0 & 0 & 0 & 0 & 0 \\ 0 & 0 & 0 & 0 & 0 & 0 \end{bmatrix} \quad (5)$$

where K_t is a 6×6 matrix in terms of the stiffnesses K_s, $\mathcal{K}_i$, and $\mathcal{K}_g$ and the finite element height h_e. (Franco et al., 2022) states that with h_e taken as $\frac{H}{3}$, it is possible to have very accurate results up to the third vibration mode. Note that M_e is a 6×6 matrix which corresponds to the mass matrix of the classical Euler-Bernoulli beam model where the rotational inertia is not involved because it is associated with much higher vibration modes in frame structures (Chesnais, 2010). The HBFEM model is a 1D beam model discretized in finite elements with 3 degrees of freedom at each node. The construction of this numerical formulation is well detailed in (Franco et al., 2022). An example code written in MatLab of the HBFEM application is available in: *https://github.com/cafariza/HBFEMmodel.git*

3. Case study: Grenoble City Hall building

The performance of the HBFEM have already been investigated in (Franco et al, 2022) for the transverse dynamics of realistic n-story n-bay plane frame structures. Herein, the validation focuses on its application on real structures. Then, the equivalent beam model construction of the Grenoble City Hall building is performed and its results are compared with the results of the (Desprez et al, 2015) full finite element model (see Fig. 3). This detailed numerical model is composed of 21102 elements and 12275 nodes.

3.1 Description of the structure

The Grenoble City Hall (GCH) is a reinforced concrete structure with a square patio of two stories crowned with a tower at one side, which is the object of this study. The tower has 11 stories above the patio building which sums 13 stories and 52 m of height from ground to top (Desprez, 2010). The tower is 43 m long and 13 m wide (Fig. 3a). The structural components are columns, 4 pillars (containing the staircases and elevator shafts) and beams. The main hall, located at the ground story, is a floor with double height where the only vertical members are the four pillars. They support a prestressed transfer slab on which the tower is built. The cross-section of the pillars decreases after the transfer slab. The inter-story height is 3.2 m for the typical stories of the tower. Every column starts in the prestressed transfer slab. The ten stories above the transfer slab have an identical structural distribution. However, the column sections slightly decrease from the 6th story above the transfer slab. In the last story (11th from the transfer slab or 13th from the ground), this distribution changes and the structural components are basically shear walls. The building has also two basements with the same column distribution as the typical stories of the tower. The material properties are summarized in Table 1. The dimensions of the structural member cross-sections considered in the geometry definition of the numerical model are shown in Table 2.
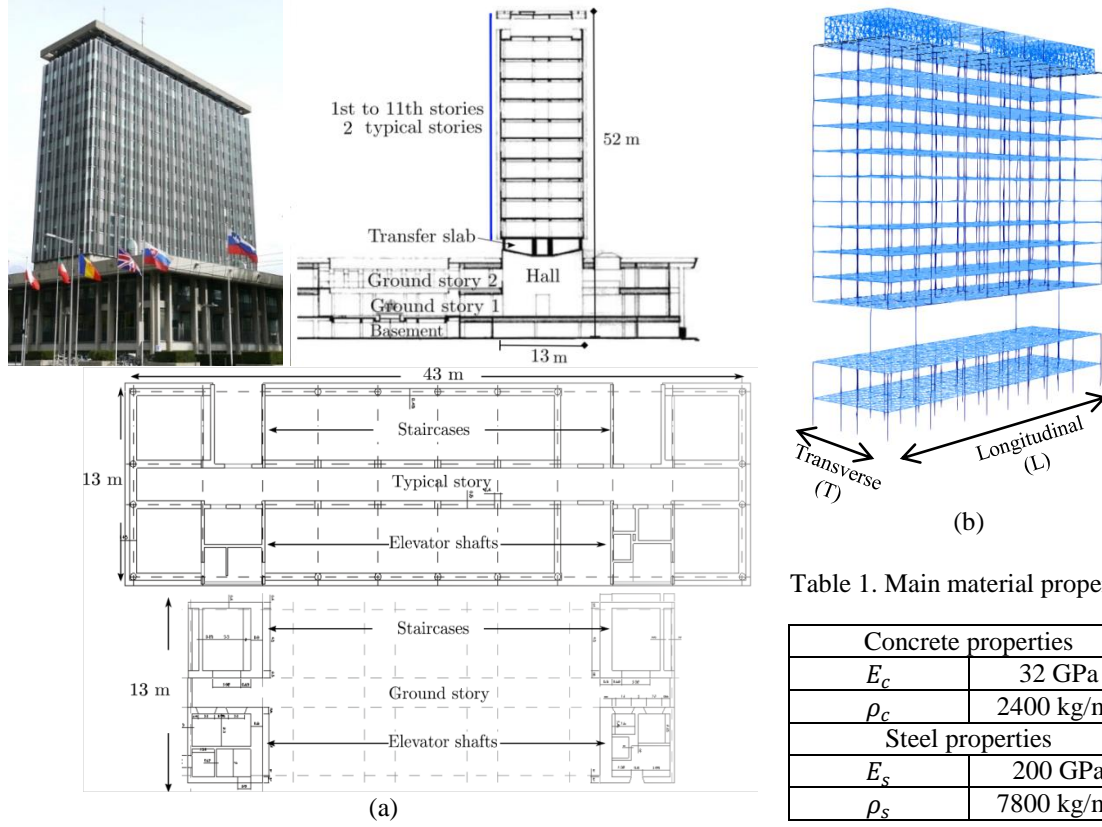
Fig. 3 The Grenoble City Hall tower block. (a) Top: General view (Jacques Mossot, 2007) and front side view of the tower block (Michel et al., 2010b). Bottom: typical story and ground story plan views. (b) Full 3D finite element model by (Desprez, 2010) (Desprez et al, 2015)

Table 1. Main material properties

Concrete properties	
E_c	32 GPa
ρ_c	2400 kg/m^3
Steel properties	
E_s	200 GPa
ρ_s	7800 kg/m^3

Table 2. Geometrical properties extracted from the detailed numerical model. [a] Average of the two basement story heights=0.5× (3.47+4.68) m.[b] 4 and [c] 3 beams in the longitudinal and transverse direction, respectively.

Property	Basement	Ground story	Typical story 1	Typical story 2
Number of stories	2	1	5	6
Story height, l (m)	4.08[a]	7.7	3.2	3.2
Slab thickness (m)	0.14	0.16	0.14	0.14
Beam sections (cm)	45×35	300 × 65[b]- 200 × 115[c]	45×35	45×35
Column sections (cm)	40×50	———	40×50	30×40
Pillar sections	R-shape	R-shape	U-shape	U-shape

3.2 Construction of the equivalent beam model

The construction of the HBFEM model for the GCH building, adopting the analytical EBM principles, requires two main steps, 1) computation of the macroscopic parameters: the linear mass Λ and the three stiffnesses $K_s, \mathcal{K}_i$, and $\mathcal{K}_g$, and 2) a matrix assembly procedure, typically performed in finite element method, to integrate the properties for each of the typical stories.

The computation of $K_s, \mathcal{K}_i$ and $\mathcal{K}_g$ is performed through:

$$\mathcal{K}_g = \sum E_{c_i} A_i d_i^2, \qquad \mathcal{K}_i = \sum E_{c_i} I_i, \qquad K_s = |\sum T|/\Delta U \qquad (6)$$

where E_c is the elastic modulus, A is the cross-section area of the vertical elements, d is the lever arm, and I refers to the second moment of area of the vertical elements. The estimation of $\mathcal{K}_g$ and $\mathcal{K}_i$ is realized in EXCEL. A table of the element's cross-sections and the concrete properties (Elastic modulus E_c and mass density ρ_c) is created to compute the

global bending inertia $I_g = A_i\, d_i^2$ and the inner bending inertia I_i. Then, $\mathcal{K}_g = \sum E_{c_i}\, A_i\, d_i^2$ and $\mathcal{K}_i = \sum E_{c_i}\, I_i$ are quickly evaluated.

The computation of the shear stiffness K_s requires a static analysis of a single story. In Equation (6), T is the shear force in each vertical element generated by a differential horizontal displacement ΔU between the bottom and the top of the story. The procedure could be done by modeling numerically one single story as explained in (Chesnais, 2010) or in (Franco et al., 2019) for plane frame structures. In this section, we intend to detail this procedure for the GCH tower.

3.2.1 Estimation of the shear stiffness K_s

To assess K_s, we need to impose the macroscopic shear deformation on a finite element model of a single story with periodic boundary conditions. We decide to perform the same analysis using two different FEM-based software, Cast3M (CEA, 2020) and ETABS (CSI, 2000), to present how to impose the periodic conditions identified by the homogenization with two different modeling strategies conditioned by the software environment.

On the one hand, the story in Cast3M is modeled with the floor at the top level supported by the vertical elements (see Fig. 4a top). On the other hand, ETABS does not allow us to impose periodic conditions, so we opted for modeling the point with a bending moment equal to zero which is located at the mid-height of the vertical elements when the rotations are periodic. In this model, the floor is at mid-level with half of the vertical elements underneath and above the floor (Fig. 4b top). The walls are modeled in both software as frame elements with their corresponding cross-sections. Here we listed the required boundary conditions for the end nodes set in Cast3M:

- All the nodes are left free to rotate but the rotations must be equal at both ends of every vertical element ($\theta_{i_{n_+}} = \theta_{i_{n_-}}$).
- The vertical displacements of all the nodes are restrained ($v_{n_+} = v_{n_-} = 0$).
- The horizontal displacements u at the level n_- are set to zero ($u_{n_-} = 0$).
- For all the nodes at the level n_+, the horizontal displacements u is equal to the ΔU (we chose $\Delta U = 3.2$m (the height of the story) for convenience).

For the ETABS story model, all the listed conditions are applicable but the periodic condition ($\theta_{i_{n_+}} = \theta_{i_{n_-}}$). The end nodes of the model, which correspond to the middle of the vertical elements, are simply set free to rotate.

Figs. 4a and 4b (bottom) present the unit cell's shear deformation in the longitudinal and transverse directions for the Cast3M and ETABS story models. The colors represent the vertical displacements. The difference between the two modeling techniques on the computation of K_s for the two typical stories is presented in Table 3. Notice that there is a small difference ($< 10\%$) for both directions using both modelling strategies. This comparison, although used only for the verification process, ensured the quality of the Cast3M results which are used herein for the rest of the computations.

3.3 The GCH building dynamic behavior

Table 4 summarizes the macroscopic parameters of all the existing stories to build the HBFEM model of the GCH tower. Note that the magnitude of the parameters slightly differs between the typical stories but, for the ground story, these values are much larger. The contrast between the stiffnesses of a story can give us an insight on the building global dynamic behavior. (Hans et al., 2008) proposes a domain criterion that identifies the mechanism or the combination of mechanisms (i.e., shear, inner bending, and global bending) that govern the building dynamics. This identification criterion is particularly

useful to select the beam model (shear beam, Timoshenko beam , or the full EBM) that can reproduce the dynamics of the analyzed structure. For the typical story 1 of the GCH tower, $\mathcal{K}_g$ is much larger than K_s and $\mathcal{K}_i$ in the longitudinal and transverse directions. This comparison indicates that the behavior of the structure in both directions combines the inner bending and shear mechanisms. This analysis identifies the same behavior for the typical story 2 and the ground story in the longitudinal direction. Favorably, the inner bending and shear mechanism can be captured by the generalized form of the EBM and, indeed, the HBFEM. This mechanical functioning is characterized by large interaction between the shear deformation of the story and the inner bending of the vertical elements, which is not possible to be described with a Timoshenko beam model, for example.

Table 3. Comparison of the shear stiffness K_s obtained with the story model in Cast3M and in ETABS.

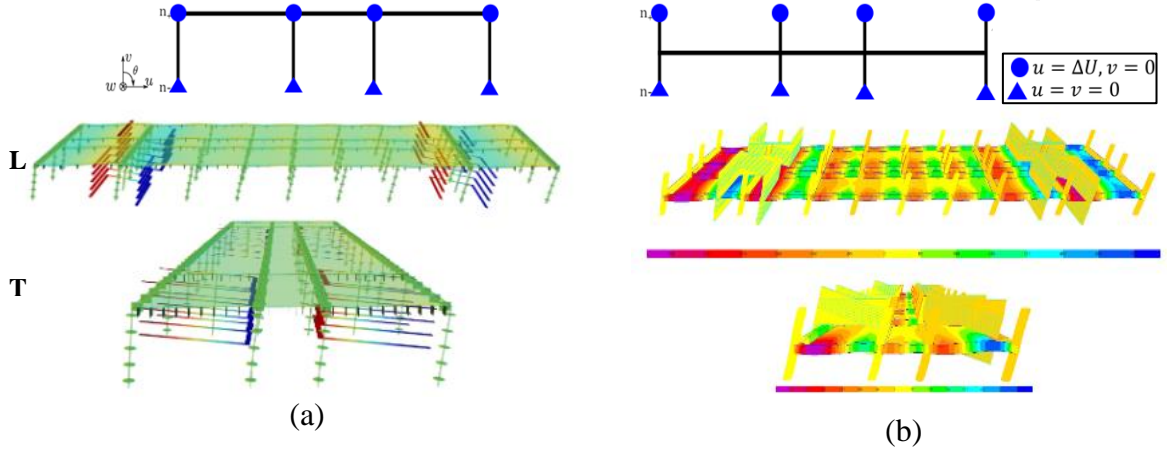| Typical story	Direction	K_s (Cast3M)[MN]	K_s (ETABS)[MN]	|% difference|
1	Longitudinal	1086.92	1024.33	5.76
	Transverse	1276.47	1459.93	9.90
2	Longitudinal	705.48	657.83	6.75
	Transverse	979.37	1043.19	6.52

Fig. 4 Boundary conditions (Top) and shear deformation (Bottom) in the Cast3M and ETABS story models. (a) Cast3M model and (b) ETABS model.

Table 4. Macroscopic parameters for the typical stories 1 and 2 in the longitudinal (L) and transverse (T) directions.

Macroscopic parameters	Typical story 1		Typical story 2		Ground story		Basement	
	L	T	L	T	L	T	L	T
Λ, linear mass (ton/m)	164		158		263.37		197.64	
K_s, shear stiffness (MN)	1086.92	1276.47	705.48	979.37	3482.47	34001.66	1391.36	1731.45
$\mathcal{K}_i$, inner bending stiffness (MN m^2)	1.66×10^6	1.51×10^6	1.66×10^6	1.51×10^6	5.26×10^6	4.71×10^6	5.26×10^6	4.71×10^6
$\mathcal{K}_g$, global bending stiffness (MN m^2)	1.36×10^8	1.01×10^7	1.24×10^8	8.74×10^6	2.62×10^8	1.68×10^7	2.94×10^8	2.02×10^7

3.4 Dynamic properties of the GCH

With the elementary stiffness K_t and mass M_e matrices (Equation (5)) totally solved, the modal analysis with the HBFEM model searches for the solution of the following eigenvalue problem:

$$KE - \omega^2 ME = 0 \tag{7}$$

where $\boldsymbol{K}$ and $\boldsymbol{M}$ are the square stiffness and mass matrices of the whole homogenized beam. E corresponds to the eigenvector and ω^2 to the eigenvalues.

Table 5 summarizes the first two eigenfrequencies $f_i = \omega_i/2\pi$ obtained for the HBFEM model in the longitudinal and transverse directions of the GCH tower. The in-situ results are shown for general information. The relative difference between the HBFEM model and the (Desprez, 2010) detailed numerical model is also presented. The overall results are satisfactory with differences no higher than 6% for the first vibration mode and slightly higher than 10% for the second vibration mode. Interestingly, the HBFEM frequencies are equal to in-situ ones for the first mode in both directions. Two main reasons can explain the discrepancies encountered for the second mode. Firstly, the accuracy of the HBFEM model directly depends on the value of the scale ratio ε. The larger ε is, the less accurate the HBFEM model is. ε becomes larger as the number of the analyzed mode increases. If the third vibration mode is estimated, it is normal to obtain even higher differences between the full detailed numerical model and the HBFEM model. Secondly, other mechanisms such as the shear acting on very thick vertical elements may emerge at the leading order, which could be the case for the walls of the staircases and elevator shafts of the GCH building (see (Chesnais, 2010)).

The computed frequency ratios $\boldsymbol{f_i/f_1}$ (1; 4.58) are different from the common values found in the literature for shear beams (1; 3; 5) or Euler-Bernoulli beams (1; 6.25; 17.36), which agrees well with the inner bending and shear behavior encountered in previous section. Fig. 5 displays the first two mode shapes in the longitudinal and transverse directions. Although a difference between the natural frequencies is observed, the mode shapes of the HBFEM and DFEM are in pretty good agreement.

Table 5. Comparison of the first two modal frequencies for the longitudinal direction

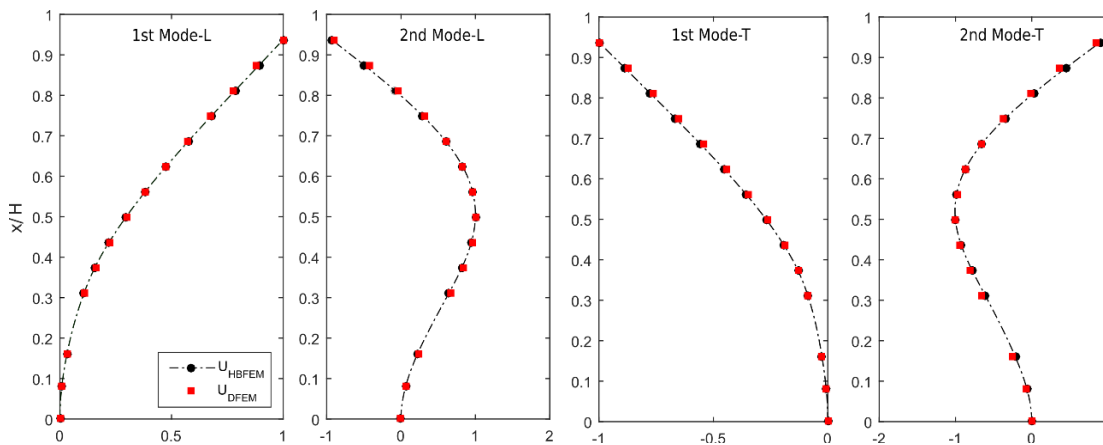| Mode-direction	HBFEM (Hz)	Ratio f_i/f_1	Detailed FEM (Hz)	Ratio f_i/f_1	In-situ (Michel, 2007)(Hz)	Ratio f_i/f_1	r. difference (%)
1-L	1.16	1	1.10	1	1.16	1	5.45
2-L	5.31	4.58	4.71	4.23	4.50	3.88	12.74
1-T	1.22	1	1.19	1	1.22	1	2.52
2-T	5.47	4.48	5.00	4.21	Not reported	-	9.40

Fig. 5 Comparison of the first two mode shapes obtained with the HBFEM model (black) and the detailed numerical model DFEM (red) for the longitudinal (left) and transverse (right) directions. The mode shapes are normalized with respect to the maximum displacement.

3.5 Seismic response through a time history analysis

A transient dynamic analysis of the GCH tower on the longitudinal direction is now performed using Newmark's time integration scheme with the constant average acceleration assumption. The viscous term $\boldsymbol{C}$ in Equation (4) corresponds to the Rayleigh

damping matrix for this computation with 5% of the critical damping for the first two longitudinal modes. The seismic input corresponds to the north-south component of the ground accelerogram of the earthquake event recorded on August 2, 2017 in Ibaraki, Japan (see Fig. 6 a). Its magnitude is M_w = 5.1 and the peak acceleration is 0.13 g with most of the energy content between 5 and 10 Hz. A total duration of 45 s and a time step of 0.01s are considered. Figs.6c and 6d display the two simulations of the top roof displacement of the structure with respect to time and their amplitude Fourier spectrum, respectively. The results show a satisfactory agreement in terms of both time and spectral amplitudes. Nonetheless, the HBFEM model provides a maximum displacement value slightly higher than the one obtained with the detailed model (6.52 mm vs 4.82 mm). On the spectra of Fig. 6d the peaks of the first two frequencies (around 1.16 Hz and 5.31 Hz) are well pronounced and their amplitudes agree for both models. These results are encouraging and show that the HBFEM model provides very good estimations of the structural response at lower computational costs. Once the geometry is defined in MatLab for the HBFEM model and in Cast3M for the detailed FEM model, the computation time of the dynamic analysis with the same resources could easily be two thousand times longer for the detailed FEM model (3s versus 100 min).
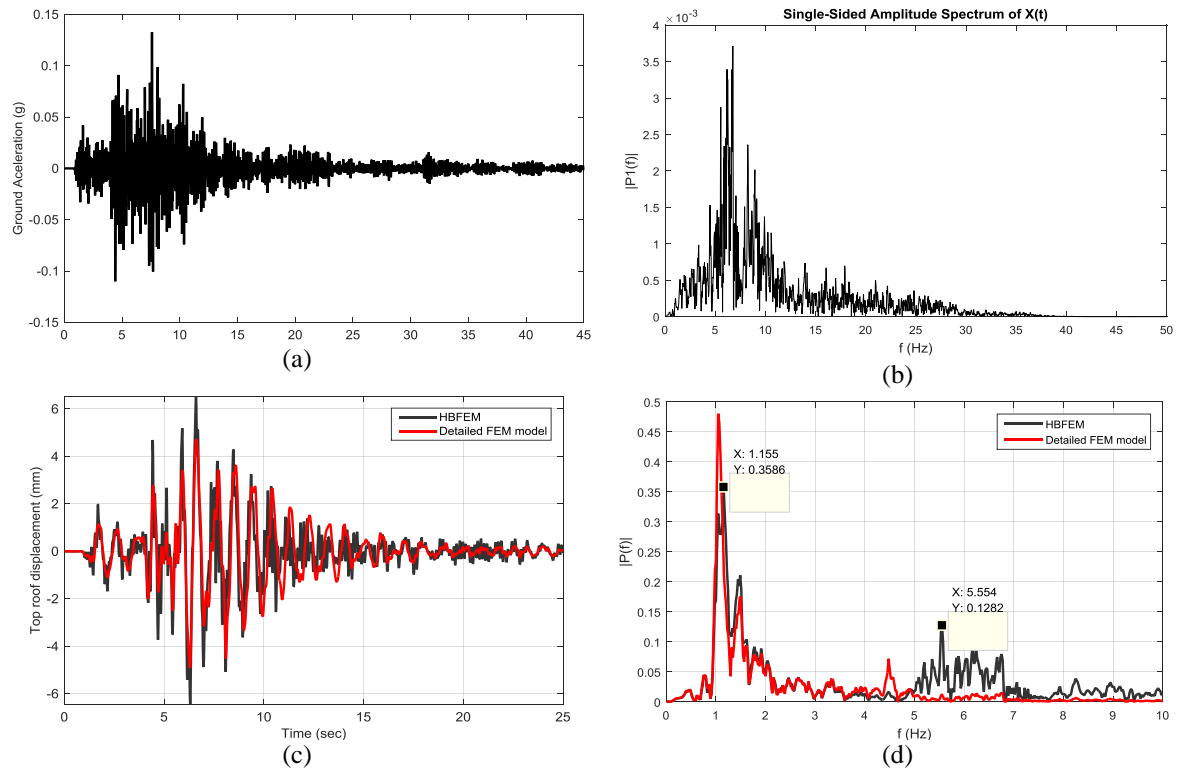

Fig. 6 Time history analysis results. (a) Ground acceleration record (N-S component). (b) Amplitude spectrum. (c) Top roof displacements and (d) amplitude spectra for the HBFEM model (black) and the (Desprez, 2010) detailed numerical model (red).

4. Conclusions

This study clearly shows the numerical performance of the homogenized beam finite element model built with the EBM basis. An accurate description of the dynamics of the Grenoble City Hall tower is possible with the use of this 1D model approach. The study of the GCH tower validates the proposed strategy for analyzing a structure with different typical stories through the substructure assembly procedure and widens the application domain of the HBFEM model. The eigenfrequencies and mode shapes are estimated with

the HBFEM model and compared with the results of the full detailed numerical model. A good agreement between both models is obtained for the first two flexural modes in each direction. A time history analysis is also performed. The results show a satisfactory agreement in terms of both time and spectral amplitudes in the lower frequency range. It was also possible to identify that the leading mechanism for the GCH structure corresponds to a combination of the inner bending and the shear of the story in both longitudinal and transverse directions. Further works will be dedicated to the integration of the HBFEM in slight non-linear analyses.

Acknowledgements

References

− Boutin, C. and Hans, S. (2003). Homogenisation of periodic discrete medium: Application to dynamics of framed structures. Computers and Geotechnics, 30(4):303–320.

− Boutin, C., Hans, S., and Chesnais, C. (2010). Generalized Beams and Continua. Dynamics of Reticulated Structures, pages 131–141. Springer New York, New York, NY.

− Caillerie, D., Trompette, P., and P., V. (1989). Homogenisation of periodic trusses. pages 303–320.

− CEA, Cast3M v. 17. http://www-cast3m.cea.fr/ (2017). http://www-cast3m.cea.fr/.

− Chesnais, C. (2010). Dynamique de milieux réticulés non contreventés : application aux bâtiments. Thesis, Ecole Centrale de Lyon.

− Chesnais, C., Boutin, C., and Hans, S. (2011a). Structural Dynamics and Generalized Continua, pages 57–76. Springer Berlin Heidelberg, Berlin, Heidelberg.

− CSI, "ETABS Integrated Software for Structural Analysis and Design," Computers and Structures Inc., Berkeley, California.

− Desprez, C. (2010). Analyse et Réduction de la Vulnérabilité Sismique des Structures Existantes : Renforcement par Collage de Tissus de Fibres de Carbone (TFC). Thesis, Institut National Polytechnique de Grenoble - INPG.

− Desprez, C., Kotronis, P., and Mazars, J. Seismic vulnerability assessment of a RC structure before and after FRP retrofitting. Bull Earthquake Eng 13, 539–564 (2015). https://doi.org/10.1007/s10518-014-9621-1

− Franco, C., Chesnais, C., Semblat, J.-F., Desprez, C., and Giry, C.(2019). Une technique d'homogénéisation appliquée aux bâtiments périodiques multiportiques. In 10ème colloque national de l'AFPS - AFPS'19, Strasbourg, France.

− Franco, C., Chesnais, C., Semblat, J.-F., Giry, C., and Desprez, C. (2022). Finite element formulation of a homogenized beam for reticulated structure dynamics. Computers & Structures, 261-262:106729. https://doi.org/10.1016/j.compstruc.2021.106729

− Hans, S. and Boutin, C. (2008). Dynamics of discrete framed structures: a unified homogenized description. Journal of Mechanics of Materials and Structures, 3(9):1709–1739.

− Michel, C. (2007). Vulnérabilité Sismique de l'échelle du bâtiment à celle de la ville - Apport des techniques expérimentales in situ - Application à Grenoble. Theses, Université Joseph-Fourier - Grenoble I.

− Michel, C. and Gueguen, P. (2006). Dynamic behaviour of the first instrumented building in France: The grenoble town hall. first european conference on earthquake engineering and seismology

− Michel, C., Guéguen, P., El Arem, S., Mazars, J., and Kotronis, P. (2010b). Full-scale dynamic response of an RC building under weak seismic motions using earthquake recordings, ambient vibrations and modelling. Earthquake Engineering & Structural Dynamics, 39(4):419–441.